

COMPARISON OF CONNECTIVITY ANALYSES FOR RESTING STATE EEG DATA

Elzbieta Olejarczyk^{1*}, Laura Marzetti^{2,3}, Vittorio Pizzella^{2,3} and Filippo Zappasodi^{2,3}

1. Nalecz Institute of Biocybernetics and Biomedical Engineering, Polish Academy of Sciences, Warsaw, Poland

2. Department of Neuroscience, Imaging and Clinical Sciences, 'G. d'Annunzio' University, Chieti, Italy

3. Institute for Advanced Biomedical Technologies, 'G. d'Annunzio' University, Chieti, Italy

*Corresponding author:

Dr. Elzbieta Olejarczyk

Email: eolejarczyk@ibib.waw.pl

Abstract

Objective. In the present work, a nonlinear measure (transfer entropy, TE) was used in a multivariate approach for the analysis of effective connectivity in high density resting state EEG data in eyes open and eyes closed. Advantages of the multivariate approach in comparison to the bivariate one were tested. Moreover, the multivariate TE was compared to an effective linear measure, i.e. directed transfer function (DTF). Finally, the existence of a relationship between the information transfer and the level of brain synchronization as measured by phase synchronization value (PLV) was investigated.

Approach. The comparison between the connectivity measures, i.e. bivariate versus multivariate TE, TE versus DTF, TE versus PLV, was performed by means of statistical analysis of indexes based on graph theory.

Main results. The multivariate approach is less sensitive to false indirect connections with respect to the bivariate estimates. The multivariate TE differentiated better between eyes closed and eyes open conditions compared to DTF. Moreover, the multivariate TE evidenced non-linear phenomena in information transfer, which are not evidenced by the use of DTF. We also showed that the target of information flow, in particular the frontal region, is an area of greater brain synchronization.

Significance. Comparison of different connectivity analysis methods pointed to the advantages of nonlinear methods, and indicated a relationship existing between the flow of information and the level of synchronization of the brain.

Keywords: EEG, resting state, functional and effective connectivity, multivariate transfer entropy, directed transfer function, phase-locking value, graph theory

1. Introduction

In recent decades, it has become clear that an adequate knowledge of brain functioning can be obtained only by understanding the brain as a structurally and functionally integrated system (Sporns et al 2000, 2005, Bassett and Bullmore 2006, 2009, Stam 2007a, 2010, 2016, Bullmore and Sporns 2009, He and Evans 2010, Friston 2011, Sporns 2011, 2013). In particular, a high performance of the brain depends on the dynamic communication between its subsystems (Tononi et al 1994, Sporns et al 2000, Bassett and Gazzaniga 2011). Indeed, for complex systems with modular topologies and oscillatory dynamics, such as the brain, a generic mechanism to dynamically route information has been proposed, in which the properties of the individual unit, the topology of the network and the external inputs co-act to systematically organize information routing (Kirst et al 2016). In this scenario, the functional connectivity, i.e. the statistical dependence between the time series from different brain areas, has been often interpreted as the mechanism underlying the information transfer among different cerebral areas. Moreover, the additional knowledge about the ‘causal’ interactions between (or among) the activities of different brain regions has been interpreted as a measure of the direction of the information transfer between (or among) them. For example, in the study of brain dysfunction, the alterations of the structural links and of the functional interactions, as well as the changes of the direction and strength of causal links is often interpreted as changes in information transfer induced by the pathology (De Vico Fallani et al 2007, Ponten et al 2007, Stam et al 2007b, Bullmore and Sporns 2009, Sanz-Arigita et al 2010, Van den Heuvel and Hulshoff 2010, Ahmadlou and Adeli 2011, Jalili and Knyazeva 2011, Zhang et al 2011, Micheloyannis 2012, Wang et al 2013, Chiang et al 2014, Van den Heuvel and Fornito 2014, Vecchio et al 2014). Nevertheless, the relationship between functional and directed connectivity metrics and measures of information transfer is still debated. Among neuroimaging techniques, electroencephalography (EEG) and magnetoencephalography (MEG) allow us to follow the neural dynamics with accurate temporal resolution, and they are therefore the most suitable techniques to non-invasively track brain interactions and information transfer. So far, linear and non-linear as well as parametric and non-parametric methods, mutated from information-theoretic tools, have been applied to EEG/MEG signals to quantify the directed interactions between distributed brain activity and to characterize the information transfer during its functioning, both at rest and during task. Indeed, the temporal ordering makes it possible to infer causal relationships between two simultaneously measured time series (Wiener 1956). From a statistical point of view, Granger (1969) proposed the following definition of causality from the time series X to the time series Y : if the prediction error variance of Y at the present time is reduced by including past measurements from X , then X can be said to have a causal effect on Y . The measures of causality, first introduced by Saito and Harashima (1981), were utilized to study the relationship between a pair of EEG channels, described by directed coherence of a bivariate autoregressive process (Kamitake et al 1984, Wang and Takigawa 1992). In the case of multivariate data, a full multivariate spectral measure (directed transfer function, DTF,

Kaminski and Blinowska (1991)) has been proposed to find out the directional influences between any given pair of channels. The DTF has the advantage of requiring that only one multivariate autoregressive model is estimated from multi-channel recordings.

Recently, transfer entropy (TE) has been proposed as a general method for measuring the amount of directed, time asymmetric, transfer of information between two random processes X and Y (Schreiber 2000): the TE from X to Y is the amount of uncertainty reduced in future values of Y by knowing the past values of X and given the past values of Y. Usually, a bivariate approach has been used to calculate the TE. The reliability of TE in EEG data has been demonstrated (Faes et al 2016). Recently, Montalto et al (2014) introduced the multivariate transfer entropy, which allows for the elimination of false indirect connections characteristic of bivariate measures. In our work, we have applied for the first time the multivariate TE for the analysis of directional connectivity in high density EEG data in two resting conditions: eyes open and eyes closed. Firstly, we tested in real data the advantages of the multivariate approach in comparison with the bivariate one, i.e. the elimination of false indirect connections present in bivariate estimates.

Secondly, the multivariate TE was compared to the DTF. Indeed, the TE is a measure based on a non-parametric statistic, so it does not assume a priori any kind of model for the interaction (whether linear or nonlinear), in contrast to the Granger causality based measures, such as DTF, which depend on the autoregressive model. It has been shown that TE and Granger causality are equivalent for Gaussian variables and TE reduces to Granger causality for auto-regressive models (Barnett et al 2009). Nevertheless, TE is advantageous when the model assumption of Granger causality does not hold, e.g. in the analysis of non-linear signals (Hlavackova-Schindler et al 2007). Therefore, the significance of the comparison between TE and DTF is in line with the characterization of non-linearities of brain dynamics, previously described at different time scales (Honey et al 2007). Indeed, differences between TE and DTF could arise from the existence of nonlinearities, which are not taken into account in the autoregressive model.

In studying functional connectivity between EEG and MEG time series, phase synchronization of oscillatory brain activity has been observed in multiple defined frequency bands and has been shown to feature strong condition specific modulations, while being less constrained by structural coupling (Engel et al 2013). Indeed, Engel and collaborators introduced the concept of 'intrinsic coupling modes' (ICMs), i.e. coupling present in absence of any external stimulus. ICMs are characterized by distinct spectral and spatial signatures which change over time in a context and learning dependent manner. Two types of ICMs can be distinguished: phase coupling of band-limited oscillatory signals ('phase ICMs') and coupled aperiodic fluctuations of signal envelopes ('envelope ICMs'). Phase ICMs have been hypothesized to play a central role in neuronal communication at both local and large scale (Fries 2005, 2015) by regulating the integration and flow of cognitive contents on fast time scales relevant to behaviour (e.g. Varela et al (2001), Fries (2005, 2009, 2015), Fell and Axmacher (2011), Buzsaki and Wang (2012) and Engel et al (2013)).

The last aim of our work was to prove the existence of a relation between information transfer and the level of brain synchronization as measured by phase coupling. For this reason, TE and DTF were compared with a measure of phase synchronization, the phase locking value (PLV) (Varela et al 2001). The comparison between the connectivity measures, i.e. bivariate versus multivariate TE, TE versus DTF, TE versus PLV, was performed by means of statistical analysis of indexes based on graph theory, previously used in EEG connectivity analysis to characterize resting state brain architecture and organization under healthy conditions, as well as their changes in some neurodegenerative diseases (Stam et al 2007b, Van den Heuvel and Hilshoff 2010, Micheloyannis 2012, Chiang et al 2014, Van den Heuvel and Fornito 2014).

2. Materials and methods

2.1 EEG recording and preprocessing

Ten minute electroencephalographic (EEG) recordings were acquired in 19 healthy subjects at rest (10 males, age: 22.8 ± 3.9 years). The experimental protocol was approved by the Ethical Committee of 'G. d'Annunzio' University, in Chieti. All subjects signed a written informed consent. Subjects were sat in a comfortable armchair and rest brain activity was acquired both at eyes open, while fixating on a cross displayed on a screen, and at eyes closed. Data were sampled at 1000 Hz. The EEG activity was recorded by 128 electrodes (Electrical Geodesics, Inc.) referenced to the Cz electrode and positioned according to the 10-10 international system of electrode placement. Out of the 128 electrodes, a subset of 96 electrodes free from artefacts and common to all subjects, was retained for further analysis.

A semiautomatic procedure based on Independent Component Analysis (Barbati et al 2004) was applied to identify and eliminate artifacts (i.e. eye movements, cardiac activity and muscle contractions). Data were rereferenced to the common average which, given the high electrode number, is a reasonable choice for connectivity studies (Marzetti et al 2007, Chella et al 2016). The signal of each EEG channel was band pass filtered using a finite impulse response (FIR) filter with linear phase of order 1000 in the 1–45 Hz band (function FIR1 implemented in Signal Processing Toolbox in Matlab). Moreover, to derive narrow band time domain signals, FIR filtering in the physiological frequency bands, 2–4 Hz (delta), 4.5–7.5 Hz (theta), 8–12.5 Hz (alpha), 13–30 Hz (beta), 30–45 Hz (gamma) was applied.

2.2 Functional connectivity and information transfer measures

Transfer entropy and phase locking value were calculated for each EEG signal, band-pass filtered in the above defined frequency bands, as well as for signals in the whole spectrum (1–45 Hz). Directed

transfer function was calculated in the frequency domain. Values corresponding to the different frequency bands and to the whole spectrum were obtained as the average of DTF in the corresponding frequency intervals. DTF and PLV were calculated using the algorithms included in the Matlab Toolbox—HERMES (Niso et al 2013, <http://hermes.ctb.upm.es>). The multivariate as well bivariate TE were calculated using the MuTE Toolbox (Montalto et al 2014, <http://mutetoolbox.guru/>). For the ease of reading, we will briefly recall the theory behind each measure.

Transfer Entropy Entropy is a basic measure of information theory (Shannon 1948). Let X be a discrete random process with N outcomes: $X = \{x_1, \dots, x_N\}$ and the probability of the x_i outcome $p(x_i)$, then the average information or Shannon entropy (S) of a message about the outcome of X is:

$$S = - \sum_{x_i \in X} p(x_i) \cdot \log p(x_i) \quad (1)$$

Before introducing the concept and definition of the TE, we need to recall the concept of ‘mutual information introduced by Shannon (1948). The ‘mutual information of two variables X and Y with joint probability $p(x_i, y_i)$ is defined as:

$$M_{XY} = S_X + S_Y - S_{XY} = - \sum_{x_i \in X} p(x_i) \cdot \log p(x_i) - \sum_{y_i \in Y} p(y_i) \cdot \log p(y_i) - \sum_{x_i \in X, y_i \in Y} p(x_i, y_i) \cdot \log p(x_i, y_i) \quad (2)$$

The ‘mutual information (M) can be expressed in form of the Kullback–Leibler divergence (Cover and Thomas 1991), which is a relative entropy comparing the two probability distributions $p(x_i, y_i)$ and $p(x_i) \cdot p(y_i)$:

$$M_{XY} = \sum_{x_i \in X, y_i \in Y} p(x_i, y_i) \cdot \log \frac{p(x_i, y_i)}{p(x_i) \cdot p(y_i)} \quad (3)$$

In such form, the mutual information quantifies the deviation from independence of two variables X and Y . However, M_{XY} is symmetric under the exchange of X and Y and therefore does not contain any directional sense. Schreiber has proposed a measure of causality by measuring the deviation from the generalized Markov condition (Schreiber 2000) given by:

$$p(y_{t+1} | y_t^n, x_t^m) = p(y_{t+1} | y_t^n) \quad (4)$$

where $x_t^m = (x_t, x_{t+1}, \dots, x_{t+m-1})$ and $y_t^m = (y_t, y_{t+1}, \dots, y_{t+n-1})$ and m and n are orders of the Markov processes in X and Y , respectively. The right hand side of the equation is the probability of obtaining a value of y_{t+1} given its previous n steps, while the left hand side estimates this probability when both the histories of x_t and y_t are taken into account. This equation is fully satisfied when the transition probabilities (i.e. the dynamics) of Y are independent of the past of X , which means no causality from X to Y . Thus the deviation from this condition quantifies dependence in term of causality. To measure such deviation, the Kullback–Leibler divergence between the two probability distributions at each side of above equation, $p(y_{t+1}|y_t^n, x_t^m)$ and $p(y_{t+1}|y_t^n)$ is used (Schreiber 2000) to define the transfer entropy as in:

$$TE_{x \rightarrow y} = \sum_{y_{t+1}, y_t^n, x_t^m} p(y_{t+1}|y_t^n, x_t^m) \log \left(\frac{y_{t+1}|y_t^n, x_t^m}{y_{t+1}|y_t^n} \right) \quad (5)$$

TE measures the amount of directed information flow from X to Y .

In the calculation of TE, the selection of appropriate parameters such as the determination of the embedding dimension and delay, the embedding method and the estimator of the probability density function is important. The embedding delay is determined by finding the first zero of the autocorrelation function, while the embedding dimension is estimated by using the Cao criterion (Cao 1997), which is based on the search for false neighbors. In this study, a non-uniform embedding was applied. Such an approach consists in the iterative selection of a number of previous values of the variable that carries the maximum amount of information. The probability distribution was evaluated using binning estimator, in which the conditional entropy was calculated by determining the probability distributions for different levels of quantization (in our case six levels as in Montalto et al (2014)).

Multivariate Transfer Entropy To account for possible errors in the estimation of the information transfer resulting in false connections induced by the use of bivariate methods, i.e. the calculation of TE for all EEG channels in a pairwise fashion (Blinowska and Kaminski 2013), the multivariate version of the TE has been introduced (Montalto et al 2014).

The multivariate TE from X to Y conditioned to Z is defined as:

$$TE_{x \rightarrow y} = \sum_{y_{t+1}, y_t^n, x_t^m, \vec{z}_t^k} p(y_{t+1}|y_t^n, x_t^m, \vec{z}_t^k) \log \left(\frac{y_{t+1}|y_t^n, x_t^m, \vec{z}_t^k}{y_{t+1}|y_t^n, \vec{z}_t^k} \right) \quad (6)$$

where Z is a vector of $N - 2$ variables and N is the total number of variables.

Alternative expression for the multivariate transfer entropy can be provided in terms of a difference of two conditional entropies, or of a sum of four Shannon entropies:

$$\begin{aligned} TE_{x \rightarrow y} &= S(y_{t+1}|y_t^n, \bar{z}_t^k) - S(y_{t+1}|y_t^n, x_t^m, \bar{z}_t^k) \\ &= S(y_{t+1}, y_t^n, \bar{z}_t^k) - S(y_t^n, \bar{z}_t^k) - S(y_{t+1}, y_t^n, x_t^m, \bar{z}_t^k) + S(y_t^n, x_t^m, \bar{z}_t^k) \end{aligned} \quad (7)$$

Directed Transfer Function The directed transfer function (DTF) is a multivariate measure based on Granger causality, but defined in the frequency domain (Kaminski and Blinowska 1991).

For a multivariate k-channel process: $X(t) = (X_1(t), X_2(t), \dots, X_k(t))$, the multivariate autoregressive model takes the form:

$$X(t) = \sum_{m=1}^p A(m) \cdot X(t-m) + E(t) \quad \text{or} \quad \sum_{m=0}^p A(m) \cdot X(t-m) = E(t) \quad (8)$$

where $E(t)$ is a k-dimensional vector representing white noise; A is a square $k \times k$ matrix.

Transforming the multivariate autoregressive model to the frequency domain we obtain:

$$\begin{aligned} A(f)X(f) &= E(f), \quad \text{where } A(f) = - \sum_{m=1}^k A(m) \cdot e^{-i \cdot 2\pi \cdot f \cdot m} \\ \rightarrow X(f) &= A^{-1}(f) E(f) = H(f) E(f) \end{aligned} \quad (9)$$

The matrix of coefficients H , called the transfer matrix, contains information about all relationships between the variables, including the phase relations. The directed transfer function is defined as a normalized version of the transfer matrix:

$$DDTF_{j \rightarrow i}(f) = \frac{H_{ij}(f)}{\sqrt{\sum_{j=1}^k |H_{ij}(f)|^2}} \quad (10)$$

The following relation should be satisfied to guarantee the quality of fitting of the model (Blinowska and Kaminski 2006):

$$\frac{k \cdot d}{N} < 0.1 \quad (11)$$

where N is a window length; d is the model order; and k is a number of EEG channels. The model order was estimated using the Akaike information criterion (Akaike 1974). In this paper the model order d was set to 10.

Phase Locking Value The instantaneous phase $\varphi(t)$ of a signal $x(t)$ can be estimated using the Hilbert transform $HT\{\cdot\}$ (Rosenblum et al 1997, 2001, Mormann et al 2000):

$$z(t) = x(t) + HT\{x(t)\} = A(t)e^{i\varphi(t)} \quad (12)$$

where $A(t)$ and $\varphi(t)$ are the amplitude and the phase of the signal $x(t)$. The analytic signal $z(t)$ can be understood as an embedding of the 1D time-series in the 2D complex plane.

The phase of the signal is thus computed by the following expression:

$$\varphi(t) = \arctan\left(\frac{\text{Im}\{z(t)\}}{\text{Re}\{z(t)\}}\right) = \arctan\left(\frac{HT\{x(t)\}}{x(t)}\right); \quad \varphi \in [-\pi, \pi] \quad (13)$$

Two signals, $x_1(t)$ and $x_2(t)$, the phases of which are $\varphi_1(t)$ and $\varphi_2(t)$ respectively, are said to be phase synchronized if their relative phase difference $\varphi_{1,2}(t)$ is constant, as defined below:

$$\varphi_{1,2}(t) = \varphi_1(t) - \varphi_2(t) = \text{const} \quad (14)$$

To measure phase synchronization, we used the phase-locking value (PLV) defined as:

$$PLV = \left| \sum_{j=0}^{N-1} e^{i\varphi_{1,2}(j\Delta t)} \right| \quad (15)$$

where i is the imaginary unit, Δt is the time interval between two successive samples, $1/\Delta t$ is the sampling rate of discrete time series, N is the total number of samples and $\varphi_{1,2}$ is the relative phase of the two signals. Using Euler's formula value PLV turns into:

$$PLV = \left(\left[\frac{1}{N} \sum_{j=0}^{N-1} \sin(\varphi_{1,2}(j\Delta t)) \right]^2 + \left[\frac{1}{N} \sum_{j=0}^{N-1} \cos(\varphi_{1,2}(j\Delta t)) \right]^2 \right)^{\frac{1}{2}} \quad (16)$$

The value of PLV is bounded between zero and one with zero indicating unsynchronized phases and one a constant phase difference, i. e. the synchronization of signals is perfect. The decrease of the phase-locking value between two signals indicates a loss of synchronization between them.

Graph Analysis All of the measures (bivariate and multivariate TE, DTF and PLV) were calculated in time windows of 20 s to satisfy equation (11). For each connectivity measure, matrices of significant connections (the so called adjacency matrices) were produced for every frequency band separately, as well as for whole spectrum, and used as weighted adjacency matrices. To assure the correct estimation of the

autoregressive model, the DTF was calculated in the whole frequency band, and then the adjacency matrices were identified for individual frequency bands separately. The weighted adjacency matrices were analyzed using indexes based on graph theory (Bullmore and Sporns 2009, Rubinov and Sporns 2010). In graph theory, the brain is modeled as a graph composed of nodes, representing brain regions or EEG channels, and undirected or directed links between them, representing functional connections determined by TE, DTF and PLV. The graph-based indexes were calculated by using MATLAB functions collected in the Brain Connectivity Toolbox (www.brain-connectivity-toolbox.net). For each of the obtained graphs, the following indexes were calculated (Rubinov and Sporns 2010): (1) basic measures (density, degree and strength); (2) measures of integration (characteristic path length and global efficiency); (3) measures of segregation (clustering coefficient and local efficiency); (4) measure of centrality (betweenness centrality).

Basic Measures The degree of an individual node is equal to the number of links connected to that node, which, in practice, is also equal to the number of neighbors of the node. Individual values of the degree therefore reflect the importance of a node in the network. The mean network degree is commonly used as a measure of the graph density, or of the total ‘wiring cost’ of the network. The directed variant of the degree distinguishes the number of inward links from the number of outward links, while the weighted variant of the degree, termed the strength, is defined as the sum of all neighboring link weights.

Measures of integration Measures of integration estimate the ease of communication between distributed nodes. Specifically, the characteristic path length is defined as the average shortest path length between all pairs of nodes in the network, while the global efficiency is defined as the average inverse shortest path length. The global efficiency is an appropriate measure in the case of disconnected networks because the paths between disconnected nodes have infinite length, and thus zero efficiency.

Measures of centrality Measures of centrality allow for the identification of the central nodes connecting the various brain regions and hence are important for the functional integration of the brain. Betweenness centrality is defined as the fraction of all shortest paths in the network that pass through the given node.

2.3 Statistical analysis

In the adjacency matrix, only the connectivity values above the statistical threshold were considered, while non-statistically significant values were set to zero. The significance of the connectivity values was determined by surrogate data analysis (Theiler et al 1992). The surrogate data method consists in maintaining the amplitudes while destroying the phase relationship between the original signals by randomly shuffling the data in the frequency domain and then transforming them back to the time domain. The significance was tested by comparing values from the original data to values obtained from surrogate data. The number of surrogates, which were calculated for every signal, was 100.

To evidence different connectivity patterns between the two physiological conditions (eyes open and eyes closed) a three-way ANOVA model with factors: *Condition* (eyes open; eyes closed), *Band* (delta; theta; alpha; beta; gamma) and *EEG channels* (system of 96 channels), was separately applied to the following indexes for each metric: degree, strength, local efficiency and betweenness centrality. Moreover, a two-way ANOVA model with variables: *Condition* and *EEG channels*, was analyzed for the same indexes in every band separately. A two-way ANOVA model with variables: *Condition* and *Band*, was analyzed for density, characteristic path length, clustering coefficient and global efficiency.

3. Results

The functional connectivity and information transfer measures were compared under different aspects such as: (1) multivariate versus bivariate approach for TE; (2) linear versus nonlinear approach (i.e. TE versus DTF); (3) TE versus a phase connectivity measure (PLV). In figure 1, the comparison between the adjacency matrices obtained from the various approaches is shown in the two conditions (eyes open and eyes closed) for the alpha band, i.e. the most represented band in the EEG spectrum at closed and open eyes of a healthy awake adult subject, as well as for the whole spectrum between 1 to 45 Hz. To be noted that the PLV matrix is symmetrical, since PLV, differently from TE and DTF, is not a directional connectivity method, so the phase locking value locking between the *i*-th and the *j*-th channel is the same as the value between the *j*-th and *i*-th channel.

In general, the values for multivariate TE are lower than those obtained by the bivariate TE. Moreover, in the adjacency matrices the existence of many other connections can be seen in bivariate TE as compared to the multivariate TE, which may indicate that they are spurious (Blinowska and Kaminski 2013) (figure 1). The local flows between the adjacent electrodes can be noticed for nonlinear measures (diagonals in adjacency matrices of TE and PLV in figure 1).

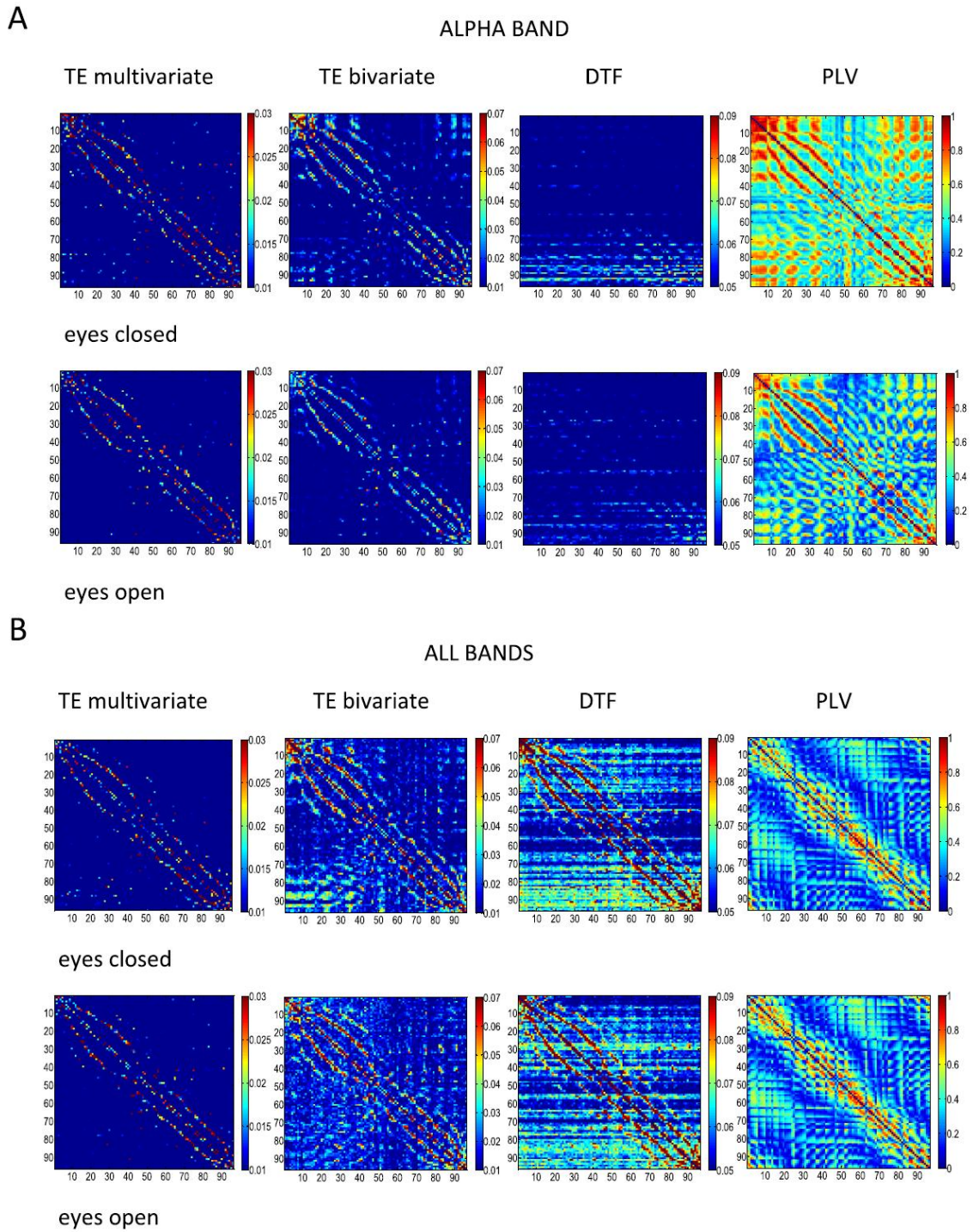


Figure 1. Adjacency matrices of the information transfer and connectivity measures (TE, DTF and PLV) in alpha band (A) and in the whole spectrum between 1–45 Hz (B) at eyes closed and eyes open.

During the resting state with eyes closed the information flows from the posterior to the frontal part of brain (the horizontal lines seen at electrodes 79–81, 85–89 and 92–95 in DTF matrix and a cluster of points seen in the lower left corner of the adjacency matrix of multivariate TE at electrodes 86–88 and 92–93; figure 1(A)). Interestingly, the horizontal cluster of points was not only seen for alpha band, but also in

the whole spectrum (figure 1(B)), although differences in the two resting states are observed mainly in the alpha frequency range. In particular, we observed a long-distance flow of information from the back to the front part of the brain in the alpha band (figure 2). Moreover, we observed that the target of the information flow (the frontal part of the brain) is a region of greater synchronization (figure 2).

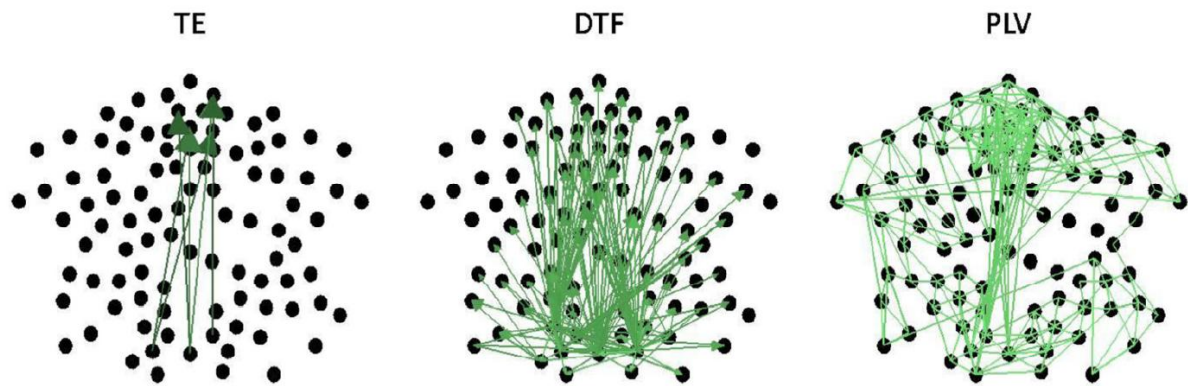


Figure 2. Graphs of information transfer and connectivity measures (TE, DTF and PLV) in alpha band at eyes closed. The circles represent the EEG channels (frontal region on top, occipital region on bottom). Significant values are represented by arrows connecting two channels (directional measures: TE and DTF) or lines (non directional measures: PLV).

Considering the graph indexes, TE and PLV allow for better discrimination between the two states (eyes open, eyes closed) than linear method, just as DTF. All indexes were higher during the resting state with eyes closed than with eyes open in alpha band. The results of ANOVA analysis for interaction *Condition* × *Band* are summarized in table 1. The arrow up/down stand for increase/decrease of index in condition eyes closed compared to condition eyes open.

Closing of eyes causes the increase of integration measures, characteristic path length (*Condition* × *Band* interaction— TE: $F(1, 34) = 5.202, p = 0.029$; PLV: $F(1, 36) = 5.308, p = 0.027$) and global efficiency (TE: $F(1, 34) = 8.576,$

$p = 0.006$; PLV: $F(1, 36) = 11.356, p = 0.002$), as well as the increase of segregation measures, clustering coefficient (TE: $F(1, 34) = 3.874, p = 0.051$; PLV: $F(1, 36) = 10.347, p = 0.0027$) and local efficiency (TE: $F(1, 3264) = 13.480, p = 0.00025$; PLV: $F(1, 3456) = 807.83, p < 0.0001$). A statistically significant increase of betweenness centrality for TE was seen also ($F(1, 3264) = 37.444, p < 0.00001$), mainly in the posterior part of brain. The higher values of betweenness centrality were found for the state with eyes closed than for the state with eyes open. For DTF only the characteristic path length was found to be different between the two rest conditions in alpha band ($F(1, 36) = 5.168, p = 0.029$, table 1).

Table 1. The results of ANOVA analysis for interaction *Condition* × *Band* and post-hoc comparisons. The arrow up/down stand for increase/decrease of index in condition eyes closed compared to condition eyes open.

GRAPH-BASED PARAMTETER	CONNECTIVITY MEASURES			
	Bivariate transfer entropy	Multivariate transfer entropy	Directed transfer function	Phase locking value
Density	—	↑ alpha	—	↑ alpha
Strenght	↑ alpha, beta	↑ alpha	—	↑ alpha, beta,gamma
Degree	↑ alpha, beta	↑ alpha	—	↑ delta, alpha, beta,gamma
Characteristic path length	—	↑ alpha	↑ alpha	↑ alpha
Global efficiency	↑ alpha	↑ alpha	—	↑ alpha
Clustering coefficient	↑ alpha	↑ alpha	—	↑ alpha
Local efficiency	↑ alpha, beta	↑ alpha	—	theta, alpha, beta, gamma
Betweenness centrality	↑ alpha, beta, gamma ↓ delta, theta	↑ delta, alpha, gamma ↓ theta	—	—

To investigate the topographic differences between the two conditions, a one-way ANOVA model, with variable *Condition*, was analyzed for each EEG channel in every band separately. The biggest differences between the two conditions (eyes open and eyes closed) were seen in alpha band for the strength. The set of electrodes, for which the statistically significant differences between conditions occurred, was illustrated in figure 3. The circles colors denote respectively: red for strength significantly greater during the resting state with eyes closed than in the resting state with eyes open; grey for electrodes escluded due to artifacts.

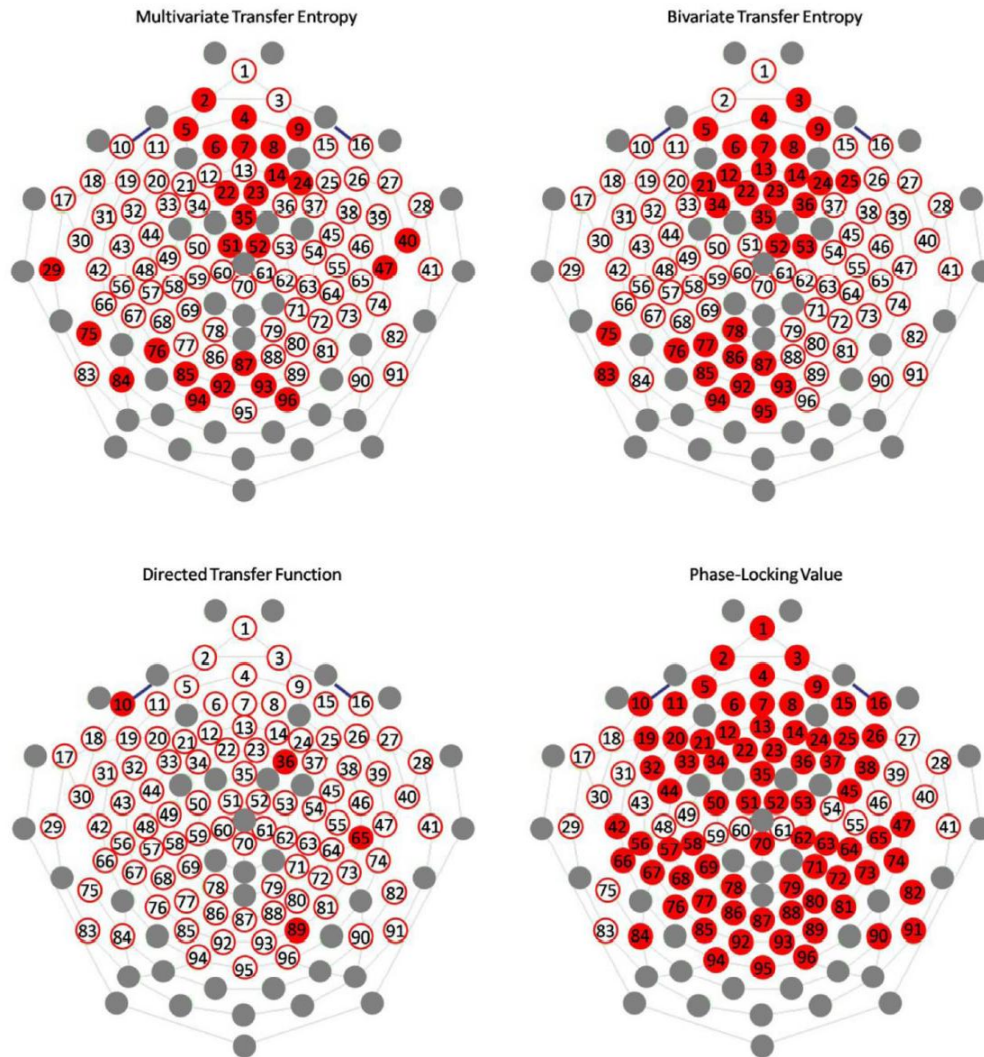


Figure 3. Topographic differences between strength of the various information transfer and connectivity measures in alpha band at eyes closed with respect to eyes open. The circles represent the channel layout, following the color code: red, strength greater during the resting state with eyes closed than in the resting state with eyes open; grey, electrodes excluded due to artifacts.

The DTF did not provide significant results in the ANOVA design for strength and degree. Conversely, the strength and the degree of alpha band increase during eyes closure for both of the two nonlinear measures. For the strength, the following results were obtained: multivariate TE: $F(1, 3264) = 192.44$, $p < 0.0001$; bivariate TE ($F(1, 3264) = 201.04$, $p < 0.0001$), PLV: $F(1, 3456) = 709.50$, $p < 0.0001$. For the degree, we obtained: multivariate TE: $F(1, 3264) = 78.774$, $p < 0.0001$; bivariate TE ($F(1, 3264) = 96.675$, $p < 0.0001$), PLV: $F(1, 3456) = 473.93$, $p < 0.0001$. Moreover, for TE and PLV strength and degree, the topography of significant differences between eyes open and eyes closed highlight brain regions located in the anterior and posterior lobe in the information flow.

The increase of indexes depending on the EEG channel (strength, degree and local efficiency) in other bands was observed only for bivariate measures (bivariate TE and PLV), which may be false connections (see table 1).

4. Discussion

In the present work, a nonlinear measure (transfer entropy) was used in a multivariate approach for the analysis of EEG signals in the resting state. The comparison between the multivariate approach and the bivariate ones evidenced higher values of the bivariate TE in comparison to the corresponding values obtained by the multivariate TE, possibly due to the Figure 3. Topographic differences between strength of the various info existence of many spurious connections in the bivariate TE, as observable in the corresponding adjacency matrices. Some authors previously underlined the potential pitfalls such as the effect of common input, due to the application of bivariate methods (Blinowska and Kaminski 2013, Kaminski et al 2016). Indeed, since EEG signals are hugely interdependent, spurious connections may be generated in applying bivariate measures to estimate connectivity from them. In Montalto et al (2014) the reliability of the multivariate transfer entropy has been extensively demonstrated on synthetic data obtained from the simulation of several physiological timeseries interacting according to given autoregressive model.

The advantage of multivariate transfer entropy with respect to other multivariate approaches consists in the fact that it is a measure that reveals any kind of dependency (linear or nonlinear). In contrast to measures based on the Granger causality, such as DTF, the transfer entropy is a nonparametric measure which is thus independent from the order of the autoregressive model. Both transfer entropy and Granger causality are equivalent for Gaussian variables (Barnett et al 2009).

In our results, differences were found between multivariate TE and DTF. In particular, TE graph indexes allow for better differentiation of activity in resting state with eyes closed and with eyes open than DTF. These results support the existence of non-linearity in brain dynamics, as previously described in the study of EEG brain dynamics (Theiler et al 1992, Kantz and Schreiber 1997, Stam et al 1999, Klonowski et al 2000, 2002, Andrzejak et al 2001, Lehnertz et al 2001, 2000, Linkenkaer-Hansen et al 2001, Stam 2005, 2006, Olejarczyk et al 2009, Rubinov et al 2009, Olejarczyk 2011, Zappasodi et al 2014, 2015).

Some studies were previously performed to find differences in connectivity patterns from EEG data in specific frequency bands in both eyes open and eyes closed resting state (Ito et al 2005, Chen et al 2013, Tan et al 2013). Connectivity was estimated by means of methods giving un-directed connectivity patterns, for example phase-based metrics (Ito et al 2005, Tan et al 2013, Miraglia et al 2016), or ICA-based approaches (Chen et al 2013), or measures coming from Information theory (Jin et al 2014). Differently, the multivariate TE allowed to the estimation of directions of the information flow. In our data, we found that

in alpha band the information flows from the posterior to the anterior part of the brain. These findings are consistent with previous EEG results for DTF (Blinowska and Kaminski 2013) as well as MEG results for phase transfer entropy (Hillebrand et al 2016). Moreover, simultaneous EEG/fMRI recordings showed that the BOLD correlates of global EEG synchronization in the alpha frequency band are located in brain areas involved in specific resting state networks (RSN, Jann et al (2009)), in particular in nodes of the default mode network (DMN). It is known that alpha oscillations are involved in the synchronization of internal mental processes, as opposed to the processing of external stimuli (Knyazev et al 2011, Marzetti et al 2014, Xu et al 2014) and likewise the DMN is characterized by increased activation at rest and decreased activation during task performance (Jann et al 2009, Pyka et al 2009, Mo et al 2013). The topography of alpha flows that we evidenced, from the central posterior to central frontal regions, is consistent with two core nodes of the DMN: the posterior cingulate cortex and the medial prefrontal cortex. It could be the result of a wide-range corticothalamic network coordinating the activity of specific nodes of the DMN. This hypothesis is in line with the results of other authors (Jann et al 2009, Hillebrand et al 2016). For instance, Hillebrand et al demonstrated that the posterior DMN is strongly activated during the resting state in the alpha and beta bands. The information flows predominantly from the posterior part of brain (visual cortex and posterior default mode network) to the anterior part of brain (anterior cingulate, frontal and temporal regions).

A relationship between phase synchronization and information flow was observed in our data. Indeed, our results showed that the target of information flow, as quantified by multivariate TE, in particular the frontal region, is an area of greater brain synchronization, evidenced by high values of PLV. The existence of a relationship between phase synchronization and transfer entropy has been noticed analyzing the spatial propagation of transient phase resetting induced by transcranial magnetic stimulation (TMS) applied to the occipital area during resting state with eyes closed (Kawasaki et al 2014). The authors concluded that the emergence of the delayed phase-locking in the target area following the TMS pulse reflects the causal information flow, because the time lags between both measures were almost coincident. Moreover, it was demonstrated theoretically that the properties of the phase lag, in conjunction with the activity-dependent synaptic modification in the neural systems, may drive the changes of the direction of information flow in a neural network (Zochowski and Dzakpasu 2004). The authors investigated properties of phase synchronization in a system of two coupled non-identical Rössler oscillators and a system of non-identical Hindmarsh–Rose models of thalamocortical neurons. They observed that the synchronization in activity of the neural systems played a crucial role during information processing. Indeed, during information processing the properties of phase synchronization can be used by the network to alter its structure and, if the synaptic modifications due to timing relations between the spiking of coupled neurons are large enough, the direction of the information flow in the network can be altered. According to previous works (MacLean et al 2014, Helfrich et al 2016, Lowet et al 2016), our results

are in line with the hypothesis that phase coupling, both locally and across distributed brain regions, could be one of the mechanisms for regulation, coordination and timing of information transfer.

Our results are in line with the findings of other authors, which applied indexes based on graph theory on rest EEG data and evidenced that the processes of cerebral integration and segregation in brain networks undergo variations with opening the eyes (Chen et al 2013, Tan et al 2013, Miraglia et al 2016). Indeed, we have found that during the resting state with eyes closed with respect to eyes open TE and PLV caused an increase in alpha band of integration measures, such as characteristic path length and global efficiency, as well as of segregation measures, such as clustering coefficient and local efficiency. A similar change was observed also for density, as well as strength and degree. Even if the graph indexes were separately studied for each frequency band (delta, theta, alpha, beta and gamma), the prominent differences between the two resting state conditions, eyes closed and eyes open, were seen only in the alpha band. It could be argued that these differences would be an effect of the well known phenomenon of the alpha power suppression, i.e. a decrease of alpha power after opening the eyes. However, the alpha suppression is localized in the parieto-occipital region (Berger 1929, Adrian and Matthews 1934, Adrian 1944, Michel et al 1992, Hari et al 1997, Williamson et al 1997, Ciulla et al 1999, Patel et al 1999, Manshanden et al 2002), while we also found the involvement of other regions, for example the frontal ones for the increase of alpha band strength. The increase of integration, segregation and strength of connections in the alpha band, observed both by means of multivariate TE and PLV, suggests that during the resting state with eyes closed a process of top-down visual image creation can take place as evidenced in previous studies (Burkitt et al 2000, Ito et al 2005). Moreover, only for PLV, we found an increase of local efficiency also in other bands (theta, beta and gamma). In the light of this result, it can be hypothesized that phase coupling at different time scales, both in lower (i.e. theta) and faster (beta and gamma) frequency bands, is a mechanism which can be recovered at rest in processing the information within densely interconnected groups of brain regions (Engel et al 2013, Marzetti et al 2013). Further ad-hoc studies are needed to properly address this point. Finally, only for TE, the differences between the two resting state conditions have been found in betweenness centrality of theta, alpha and gamma bands. In particular, the betweenness centrality has been found to be stronger in alpha and gamma bands and lower in the theta band with eyes closed than with eyes open. Thus, opening the eyes may enhance the theta band activity involved in exteroceptive processing and suppress the alpha and gamma band activity in the interoceptive network (Xu et al 2014). An opposite trend between alpha and theta band has been observed for patterns of information flow in a recent resting state MEG study. It was revealed that although information flows predominantly from posterior to anterior parts of the brain in the alpha and beta bands, an oppositely directed information flow was also observed in the theta band (Hillebrand et al 2016).

Here, we investigated connectivity directly between EEG recordings. The final goal of connectivity studies would be that of inferring interactions between brain sources that can be reconstructed by applying

an inverse method (Schoffelen and Gross 2009). Nevertheless, this approach has a high computational cost, e.g. for a 6 mm cortical sampling about six thousands source signals are obtained and have to be considered for functional connectivity estimation. This prevents the estimation of functional connectivity in source space from being a feasible approach in clinical settings where straightforwardness and real time performance are mandatory.

To derive the metrics of interest in this work, we have chosen windows of 20 s as frequently done in the EEG clinical practice (Schomer and Lopes da Silva 2012). Given the number of EEG channels and the model order for the DTF calculation, the smaller value for the window length that ensures the quality of the model fitting is 10 s. Nevertheless, if the window length is stepwise increased (10, 20, 40 s), the results of our work do not change substantially (see figure 1 in the supplementary material).

The usefulness of a connectivity method depends on some aspects such as the robustness to common inputs, noise, and volume conduction (Kaminski et al 2016). Indeed, the robustness of transfer entropy to noise and volume conduction was previously demonstrated (Vicente et al 2011). On the other hand, PLV and DTF can suffer from volume conduction and common input effects, respectively (Sadaghiani et al 2012, Baccalá and Sameshima 2001). In our results, these effects may have been mitigated by the fact that the conclusions are drawn from contrasts between the conditions. Nevertheless, to avoid any possible confounds, further studies should be done to investigate the performance of methods robust to these effects (e.g. imaginary phase locking value, Sadaghiani et al (2012)).

Finally, it should be noted that graph measures are influenced by the number of nodes and the average degree of the network (see e.g. van Wijk et al (2010) and Joudaki et al (2012)). Nevertheless, no consensus exists, to date, on the method suitable to correct for such dependencies despite the large number of proposed strategies (van Wijk et al 2010). The choice of the threshold still has to be considered as an educated guess for instance in cases when an 'optimal' connection density is set as the best statistical trade off to differentiate between the global and local structural properties of a network (Di Lanzo et al 2012). For this reason, it can be good practice to evaluate the graph metrics derived from the adjacency matrices obtained from different threshold values (Tan et al 2013, see also figure 2 in the supplementary material).

In summary, with respect to the aims of our work, we firstly confirmed in real EEG data at rest that a multivariate approach of TE in comparison with the bivariate one is less sensitive to false indirect connections with respect to bivariate estimates. Moreover, the multivariate TE evidenced non-linear phenomena in information transfer, which are not evidenced by the use of DTF. Finally, a relation between the information transfer and the level of brain synchronization as measured by phase coupling was addressed. Specifically, the target of information flow, as quantified by multivariate TE is an area of greater brain synchronization, evidenced by high values of PLV.

Acknowledgement

The authors want to acknowledge Peter Angelo Taliaferro for language editing. This work was partially supported by Faculty Resources Grant 2016, 'G. d'Annunzio' University of Chieti-Pescara 'Methods for the study of functional connectivity with MEG and EEG and applications to neuroscience' and by PRIN 20102011 No. 2010SH7H3F 006 'Functional connectivity and neuroplasticity in physiological and pathological aging'.

REFERENCES

- Adrian E D 1944 Brain rhythms *Nature* **153** 360–2
- Adrian E D and Matthews B H C 1934 The Berger rhythm: potential changes from the occipital lobes in man *Brain* **57** 355–84
- Ahmadlou M and Adeli H 2011 Functional community analysis of brain: a new approach for EEG-based investigation of the brain pathology *Neuroimage* **58** 401–8
- Akaike H 1974 A new look at the statistical model identification *IEEE Trans. Automatic Control* **19** 716–23
- Andrzejak R G, Lehnertz K, Mormann F, Rieke C, David P and Elger C E 2001 Indications of nonlinear deterministic and finite-dimensional structures in time series of brain electrical activity: dependence on recording region and brain state *Phys. Rev. E* **64** 061907
- Baccalá L and Sameshima K 2001 Partial directed coherence: a new concept in neural structure determination *Biol. Cybern.* **84** 463–74
- Barbati G, Porcaro C, Zappasodi F, Rossini P M and Tecchio F 2004 Optimization of ICA approach for artifact identification and removal in MEG signals *Clin. Neurophys.* **115** 1220–32
- Barnett L, Barrett A and Seth A 2009 Granger causality and transfer entropy are equivalent for Gaussian variables *Phys. Rev. Lett.* **103** 238701
- Bassett D S and Bullmore E T 2006 Small-world brain networks *Neuroscientist* **12** 512–23
- Bassett D S and Bullmore E T 2009 Human brain networks in health and disease *Curr. Opin. Neurol.* **22** 340–7
- Bassett D S and Gazzaniga M S 2011 Understanding complexity in the human brain *Trends Cogn. Sci.* **15** 200–9
- Berger H 1929 Uber das Elektrenkephalogramm des Menschen *Arch. Psychiatrie und Nervenkrankheiten* **87** 527–70
- Blinowska K and Kaminski M 2006 Multivariate signal analysis by parametric models handbook of time series analysis *Recent Theoretical Developments and Applications* (New York: Wiley) pp 373–411
- Blinowska K and Kaminski M 2013 Functional brain networks: random, 'small world' or deterministic? *PLoS One* **8** e78763
- Bullmore E and Sporns O 2009 Complex brain networks: graph theoretical analysis of structural and functional systems *Nat. Rev. Neurosci.* **10** 186–98
- Burkitt G R, Silberstein R B, Cadusch P J and Wood A W 2000 Steady-state visual evoked potentials and travelling waves *Clin. Neurophys.* **111** 246–58

- Buzsaki G and Wang X J 2012 Mechanisms of gamma oscillations *Annu. Rev. Neurosci.* **35** 203–25
- Cao L 1997 Practical method for determining the minimum embedding dimension of a scalar time series *Physica A* **110** 43–50
- Chella F, Pizzella V, Zappasodi F and Marzetti L 2016 Impact of the reference choice on scalp EEG connectivity estimation *J. Neural Eng.* **13** 036016
- Chen J L, Ros T and Gruzelier J H 2013 Dynamic changes of ICA derived EEG functional connectivity in the resting state *Hum. Brain Mapp.* **34** 852–68
- Chiang S and Haneef Z 2014 Graph theory findings in the pathophysiology of temporal lobe epilepsy *Clin. Neurophysiol.* **125** 1295–305
- Ciulla C, Takeda T and Endo H 1999 MEG characterization of spontaneous alpha rhythm in the human brain *Brain Topogr.* **11** 211–22
- Cover T M and Thomas J A 1991 *Elements of Information Theory* (New York: Wiley)
- De Vico Fallani F, Astolfi L, Cincotti F, Mattia D, Marciani M G, Salinari S, Kurths J, Gao S, Cichocki A and Colosimo A 2007 Cortical functional connectivity networks in normal and spinal cord injured patients: evaluation by graph analysis *Hum. Brain Mapp.* **28** 1334–46
- Di Lanzo C, Marzetti L, Zappasodi F, De Vico Fallani F and Pizzella V 2012 Redundancy as a graph-based index of frequency specific MEG functional connectivity *Comput. Math. Methods Med.* **2012** 207305
- Engel A K, Gerloff C, Hilgetag C C and Nolte G 2013 Intrinsic coupling modes: multiscale interactions in ongoing brain activity *Neuron* **80** 867–86
- Faes L, Marinazzo D, Nollo G and Porta A 2016 An information theoretic framework to map the spatio-temporal dynamics of the scalp electroencephalogram *IEEE Trans. Biomed. Eng.* **63** 2488–96
- Fell J and Axmacher N 2011 The role of phase synchronization in memory processes *Nat. Rev. Neurosci.* **12** 105–18
- Fries P 2005 A mechanism for cognitive dynamics: neuronal communication through neuronal coherence *Trends Cogn. Sci.* **9** 474–80
- Fries P 2009 Neuronal gamma-band synchronization as a fundamental process in cortical computation *Annu. Rev. Neurosci.* **32** 209–24
- Fries P 2015 Rhythms for cognition: communication through coherence *Neuron* **88** 220–35
- Friston K J 2011 Functional and effective connectivity: a review *Brain Connectivity* **1** 13–6
- Granger C W J 1969 Investigating causal relations by econometric models and cross-spectral methods *Econometrica* **37** 424–38
- Hari R, Salmelin R, Makela J P, Salenius S and Helle M 1997 Magnetoencephalographic cortical rhythms *Int. J. Psychophysiol.* **26** 51–62
- He Y and Evans A 2010 Graph theoretical modeling of brain connectivity *Curr. Opin. Neurol.* **23** 341–50
- Helfrich R F, Knepper H, Nolte G, Sengemann M, Konig P, Schneider T R and Engel A K 2016 Spectral fingerprints of large-scale cortical dynamics during ambiguous motion perception *Hum. Brain Mapp.* **37** 4099–111

- Hillebrand A, Tewarie P, van Dellen E, Yu M, Carbo E W S, Douw L, Gouw A A, van Straaten E C W and Stam C J 2016 Direction of information flow in large-scale resting-state networks is frequency-dependent *Proc. Natl Acad. Sci. USA* **113** 3867–72
- Hlavackova-Schindler K, Palus M, Vejmelka M and Bhattacharya J 2007 Causality detection based on information-theoretic approaches in time series analysis *Phys. Rep.* **441** 1–46
- Honey C J, Koetter R, Breakspear M and Sporns O 2007 Network structure of cerebral cortex shapes functional connectivity on multiple time scales *Proc. Natl Acad. Sci. USA* **104** 10240–5
- Ito J, Nikolaev A R and van Leeuwen C 2005 Spatial and temporal structure of phase synchronization of spontaneous alpha EEG activity *Biol. Cybern.* **92** 54–60
- Jalili M and Knyazeva M G 2011 EEG-based functional networks in schizophrenia *Comput. Biol. Med.* **41** 1178–86
- Jann K, Dierks T, Boesch C, Kottlow M, Strik W and Koenig T 2009 BOLD correlates of EEG alpha phase-locking and the fMRI default mode network *Neuroimage* **45** 903–16
- Jin S H, Jeong W, Lee D S, Jeon B S and Chung C K 2014 Preserved high-centrality hubs but efficient network reorganization during eyes-open state compared with eyes-closed resting state: an MEG study *J. Neurophysiol.* **111** 1455–65
- Joudaki A, Salehi N, Jalili M and Knyazeva M G 2012 EEG-based functional brain networks: does the network size matter? *PLoS One* **7** e35673
- Kaminski M J and Blinowska K J 1991 A new method of the description of the information flow in the brain structures *Biol. Cybern.* **65** 203–10
- Kaminski M, Brzezicka A, Kaminski J and Blinowska K 2016 Measures of coupling between neural populations based on Granger causality principle *Frontiers Comput. Neurosci.* **10** 114 *J. Neural Eng.* **14** (2017) 036017 E Olejarczyk *et al* 12
- Kamitake T, Harashima H and Miyakawa H 1984 A time-series analysis method based on the directed transformation *Electron. Commun. Japan* **67** 1–9
- Kantz H and Schreiber T 1997 *Nonlinear Time Series Analysis* (Cambridge: Cambridge University Press)
- Kawasaki M, Uno Y, Mori J, Kobata K and Kitajo K 2014 Transcranial magnetic stimulation induced global propagation of transient phase resetting associated with directional information flow *Frontiers Hum. Neurosci.* **8** 173
- Kirst C, Timme M and Battaglia D 2016 Dynamic information routing in complex networks *Nat. Commun.* **7** 11061
- Klonowski W, Olejarczyk E and Stepień R 2000 Nonlinear dynamics of EEG-signal reveals influence of magnetic field on the brain *Conf. Proc., IEEE Engineering in Medicine and Biology Society (Chicago)* vol 22 pp 2955–8
- Klonowski W, Olejarczyk E and Stepień R 2002 Complexity of EEG-signal in time domain—possible biomedical application *AIP Conf. Proc. (Potsdam)* vol 622 pp 155–60
- Knyazev G G, Slobodskoj-Plusnin J Y, Bocharov A V and Pyrkova L V 2011 The default mode network and EEG α oscillations: an independent component analysis *Brain Res.* **1402** 67–79
- Lehnertz K, Andrzejak R G, Arnhold J, Kreuz T, Mormann F, Rieke C, Widman G and Elger C E 2001 Nonlinear EEG analysis in epilepsy: its possible use for interictal focus localization, seizure anticipation, and prevention *J. Clin. Neurophysiol.* **18** 209–22
- Lehnertz K, Arnhold J, Grassberger P and Elger C E 2000 *Chaos in Brain?* (Singapore: World Scientific)
- Linkenkaer-Hansen K, Nikouline V V, Palva J M and Ilmoniemi R J 2001 Long-range temporal correlations and scaling behavior in human brain oscillations *J. Neurosci.* **21** 1370–7

- Lowet E, Roberts M J, Bonizzi P, Karel J and De Weerd P 2016 Quantifying neural oscillatory synchronization: a comparison between spectral coherence and phase-locking value approaches *PLoS One* **11** e0146443
- MacLean S E and Ward L M 2014 Temporo-frontal phase synchronization supports hierarchical network for mismatch negativity *Clin. Neurophysiol.* **125** 1604–17
- Manshanden I, De Munck J C, Simon N R and Lopes da Silva F H 2002 Source localization of MEG sleep spindles and the relation to sources of alpha band rhythms *Clin Neurophysiol.* **113** 1937–47
- Marzetti L, Nolte G, Perrucci M G, Romani G L and Del Gratta C 2007 The use of standardized infinity reference in EEG coherency studies *Neuroimage* **36** 48–63
- Marzetti L, Della Penna S, Snyder A Z, Pizzella V, Nolte G, de Pasquale F, Romani G L and Corbetta M 2013 Frequency specific interactions of MEG resting state activity within and across brain networks as revealed by the multivariate interaction measure *Neuroimage* **79** 172–83
- Marzetti L, Di Lanzo C, Zappasodi F, Chella F, Raffone A and Pizzella V 2014 Magnetoencephalographic alpha band connectivity reveals differential default mode network interactions during focused attention and open monitoring meditation *Front Hum. Neurosci.* **8** 832
- Michel C M, Lehmann D, Henggeler B and Brandeis D 1992 Localization of the sources of EEG delta, theta, alpha and beta frequency bands using the FFT dipole approximation *Electroencephalogr. Clin. Neurophysiol.* **82** 38–44
- Micheloyannis S 2012 Graph-based network analysis in schizophrenia *World J. Psychiatr.* **2** 1–12
- Miraglia F, Vecchio F, Bramanti P and Rossini P M 2016 EEG characteristics in ‘eyes-open’ versus ‘eyes-closed’ conditions: small-world network architecture in healthy aging and age-related brain degeneration *Clin. Neurophysiol.* **127** 1261–8
- Mormann F, Lehnertz K, David P and Elger C 2000 Mean phase coherence as a measure for phase synchronization and its application to the EEG of epilepsy patients *Physica D* **144** 358–69
- Mo J, Liu Y, Huang H and Ding M 2013 Coupling between visual alpha oscillations and default mode activity *Neuroimage* **68** 112–8
- Montalto A, Faes L and Marinazzo D 2014 MuTE: a MATLAB toolbox to compare established and novel estimators of the multivariate transfer entropy *PLoS One* **9** e109462
- Niso G, Bruna R, Pereda E, Gutierrez R, Bajo R, Maestu F and del Pozo F 2013 HERMES: towards an integrated toolbox to characterize functional and effective brain connectivity *Neuroinformatics* **11** 405–34
- Olejarczyk E 2011 Fractal dimension in time domain—application in EEG-signal analysis *Classification and Application of Fractals* (New York: Nova Science Publishers) pp 161–85
- Olejarczyk E, Sobieszek A, Rudner R, Marciniak R, Wartak M, Stasiowski M and Jalowiecki P 2009 Evaluation of the EEG signal during volatile anaesthesia: methodological approach *Biocybern. Biomed. Eng.* **29** 3–28
- Patel P, Khosla D, Al-Dayeh L and Singht M 1999 Distributed source imaging of alpha activity using a maximum entropy principle *Clin. Neurophysiol.* **110** 538–49
- Ponten S C, Bartolomei F and Stam C J 2007 Small-world networks and epilepsy: graph theoretical analysis of intracerebrally recorded mesial temporal lobe seizures *Clin. Neurophysiol.* **118** 918–27
- Pyka M, Beckmann C F, Schoning S, Hauke S, Heider D, Kugel H, Arolt V and Konrad C 2009 Impact of working memory load on fMRI resting state pattern in subsequent resting phases *PLoS One* **4** e7198

- Rosenblum M, Pikovsky A, Kurths J, Schafer C and Tass P A 2001 Phase synchronization: from theory to data analysis *Neuroinformatics* **4** 279–321
- Rosenblum M G, Pikovsky A S and Kurths J 1997 From phase to lag synchronization in coupled chaotic oscillators *Phys. Rev. Lett.* **78** 4193–6
- Rubinov M, Knock S A, Stam C J, Micheloyannis S, Harris A W, Williams L M and Breakspear M 2009 Small-world properties of nonlinear brain activity in schizophrenia *Hum. Brain Mapp.* **30** 403–16
- Rubinov M and Sporns O 2010 Complex network measures of brain connectivity: uses and interpretations *NeuroImage* **52** 1059–69
- Sadaghiani S, Scheeringa R, Lehongre K, Morillon B, Giraud A L, D'Esposito M and Kleinschmidt A 2012 Alpha-band phase synchrony is related to activity in the fronto-parietal adaptive control network *J. Neurosci.* **32** 14305–10
- Saito Y and Harashima H 1981 Tracking of information within multichannel EEG record—causal analysis in EEG *Recent Advances in EEG and EMG Data Processing* ed N Yamaguchi and K Fujisawa (Amsterdam: Elsevier)
- Sanz-Arigo E J, Schoonheim M M, Damoiseaux J S, Rombouts S A R B, Maris E, Barkhof F, Scheltens P and Stam C J 2010 Loss of 'small-world' networks in Alzheimer's disease: graph analysis of fMRI resting-state functional connectivity *PLoS One* **5** e13788
- Schoffelen J M and Gross J 2009 Source connectivity analysis with MEG and EEG *Hum. Brain Mapp.* **30** 1857–65
- Schomer D L and Lopes da Silva F 2012 *Niedermeyer's Electroencephalography: Basic Principles, Clinical Applications, and Related Fields* (Baltimore, MD: Williams & Wilkins)
- Schreiber T 2000 Measuring information transfer *Phys. Rev. Lett.* **85** 461–4
- Shannon C E 1948 A mathematical theory of communication *Bell Syst. Tech. J.* **27** 379–423
- Sporns O, Tononi G and Edelman G M 2000 Theoretical neuroanatomy and the connectivity of the cerebral cortex *Cereb. Cortex* **10** 127–41
- Sporns O, Tononi G and Kotter R 2005 The human connectome: a structural description of the human brain *PLoS Comput. Biol.* **1** e42 *J. Neural Eng.* **14** (2017) 036017
- Sporns O 2011 The human connectome: a complex network *Ann. New York Acad. Sci.* **1224** 109–25
- Sporns O 2013 Network attributes for segregation and integration in the human brain *Curr. Opin. Neurobiol.* **23** 162–71
- Stam C J, Pijn J P, Suffczynski P and Lopes da Silva F H 1999 Dynamics of the human alpha rhythm: evidence for nonlinearity? *Clin. Neurophysiol.* **110** 1801–13
- Stam C J 2005 Nonlinear dynamical analysis of EEG and MEG: review of an emerging field *Clin. Neurophysiol.* **116** 2266–301
- Stam C J 2006 *Nonlinear Brain Dynamics* (New York: Nova Science Publishers) Stam C J and Reijneveld J C 2007a Graph theoretical analysis of complex networks in the brain *Nonlinear Biomed. Phys.* **1** 3
- Stam C J, Jones B E, Nolte G, Breakspear M and Scheltens P 2007b Small-world networks and functional connectivity in Alzheimer's disease *Cereb. Cortex* **17** 92–9
- Stam C J 2010 Characterization of anatomical and functional connectivity in the brain: a complex networks perspective *Int. J. Psychophysiol.* **77** 186–94

- Stam C J, van Straaten E C, Van Dellen E, Tewarie P, Gong G, Hillebrand A, Meier J and Van Mieghem P 2016 The relation between structural and functional connectivity patterns in complex brain networks *Int. J. Psychophysiol.* **103** 149–60
- Tan B, Kong X, Yang P, Jin Z and Ling L 2013 The difference of brain functional connectivity between eyes-closed and eyes open using graph theoretical analysis *Comput. Math. Methods Med.* **2013** 976365
- Theiler J, Eubank S, Longtin A, Galdrikian B and Farmer J D 1992 Testing for nonlinearity in time series: the method of surrogate data *Physica D* **58** 77–94
- Tononi G, Sporns O and Edelman G M 1994 A measure for brain complexity: relating functional segregation and integration in the nervous system *Proc. Natl Acad. Sci. USA* **91** 5033–7
- Van den Heuvel M P and Fornito A 2014 Brain networks in schizophrenia *Neuropsychol. Rev.* **24** 32–48
- Van den Heuvel M P and Hulshoff Pol H E 2010 Exploring the brain network: a review on resting-state fMRI functional connectivity *Eur. Neuropsychopharmacol.* **20** 519–34
- Van Wijk B C, Stam C J and Daffertshofer A 2010 Comparing brain networks of different size and connectivity density using graph theory *PLoS One* **5** e13701
- Varela F, Lachaux J, Rodriguez E and Martinerie J 2001 The brainweb: phase synchronization and large-scale integration *Nat. Rev. Neurosci.* **2** 229–39
- Vecchio F, Miraglia F, Marra C, Quaranta D, Vita M G, Bramanti P and Rossini P M 2014 Human brain networks in cognitive decline: a graph theoretical analysis of cortical connectivity from EEG data *J. Alzheimers Dis.* **41** 113–27
- Vicente R, Wibral M, Lindner M and Pipa G 2011 Transfer entropy—a model-free measure of effective connectivity for the neurosciences *J. Comput. Neurosci.* **30** 45–67
- Wang G and Takigawa M 1992 Directed coherence as a measure of interhemispheric correlation of EEG *Int. J. Psychophysiol.* **13** 119–28
- Wang J, Zuo X, Dai Z, Xia M, Zhao Z, Zhao X, Jia J, Han Y and He Y 2013 Disrupted functional brain connectome in individuals at risk for Alzheimer's disease *Biol. Psychiatry* **73** 472–81
- Wiener N 1956 The theory of prediction *Modern Mathematics for Engineers* (New York: McGraw-Hill)
- Williamson S J, Kaufman L, Lu Z L, Wang J Z and Karron D 1997 Study of human occipital alpha rhythm: the alphon hypothesis and alpha suppression *Int. J. Psychophysiol.* **26** 63–76
- Xu P *et al* 2014 Different topological organization of human brain functional networks with eyes open versus eyes closed *Neuroimage* **90** 246–55
- Zappasodi F, Marzetti L, Olejarczyk E, Tecchio F and Pizzella V 2015 Age-related changes in electroencephalographic signal complexity *PLoS One* **10** e0141995
- Zappasodi F, Olejarczyk E, Marzetti L, Assenza G, Pizzella V and Tecchio F 2014 Fractal dimension of EEG activity senses neuronal impairment in acute stroke *PLoS One* **9** e100199
- Zhang J, Wang J, Wu Q, Kuang W, Huang X, He Y and Gong Q 2011 Disrupted brain connectivity networks in drug-naive, first-episode major depressive disorder *Biol. Psychiatry* **70** 334–42
- Zochowski M and Dzakpasu R 2004 Conditional entropies, phase synchronization and changes in the directionality of information flow in neural systems *J. Phys. A: Math. Gen.* **37** 3823–34